Effect of faceting on grain boundary motion in Zn

Vera G. Sursaeva [a], Boris B. Straumal [a], Alena S. Gornakova [a], Lasar S. Shvindlerman [b], Günter Gottstein [b,*]

[a] *Institute of Solid State Physics, Russian Academy of Sciences, 142432 Chernogolovka, Moscow District, Russia*
[b] *Institut für Metallkunde und Metallphysik, RWTH Aachen, Kopernikusstrasse 14, D-52056 Aachen, Germany*

Abstract

The impact of faceting on the motion of a high-angle grain boundary (GB) in Zn was studied. The steady-state motion of a $[10\bar{1}0]$ tilt GB half-loop was recorded in situ. Above 673 K the migrating GB half-loop was continuously curved. Below this temperature a facet appeared and coexisted with the curved GB. The length of the facet increased with decreasing temperature. The temperature dependence of the facet length and the steady-state motion of the GB half-loop with and without facet was investigated. A theory for the motion of a faceted GB is presented. It allows us to account for the observed phenomena and to extract the mobility and the temperature dependence of a moving facet.
© 2008 Acta Materialia Inc. Published by Elsevier Ltd. All rights reserved.

Keywords: Grain boundary; Steady-state motion; Facets

1. Introduction

The surface of minerals is often composed of planar faces which are referred to as facets. Facets are due to the crystalline nature of the materials and reflect an anisotropy of the surface energy. However, facets are not only observed on crystal surfaces but can also occur on internal interfaces, such as grain boundaries (GBs), and appear as straight GB segments in an optical micrograph. Prominent examples are coherent twin boundaries in low stacking fault energy materials [1].

The relation between GB faceting and GB behaviour, in particular, grain growth and GB migration has been subject of investigation in the past [2–5]. However, only recently quantitative methods have been put forward to tackle this problem [6–8]. The migration of incoherent twin GBs with facets was studied by Straumal et al. [7]. It was demonstrated that the rather complicated kinetics of GB motion, in particular the strong non-Arrhenius temperature dependence, could be explained by considering the

motion of two competitive facets. Rabkin considered the influence of GB faceting on grain growth and the motion of a two-dimensional (2D) GB half-loop [8]. Using several simplifying assumptions he showed that faceting might modify the von Neumann–Mullins relationship for 2D grain growth; it was also found that the length of a facet on a half-loop depended on its mobility, i.e. the length of a facet increased with rising facet mobility. The shape and the mobility of a moving GB were considered by a combination of both thermodynamic and kinetic parameters, and the driving force for facet migration was described in terms of a weighted mean curvature [9,10].

In the current study, we have investigated the influence of a facet on the curvature-driven steady-state motion of a GB in a Zn bicrystal. The experimental results are complemented by and compared to a theoretical treatment of the motion of a faceted GB.

2. Experimental

Flat bicrystals with a $[10\bar{1}0]$ direction perpendicular to the surface were grown from 99.999 wt.% pure Zn using a

---

* Corresponding author.
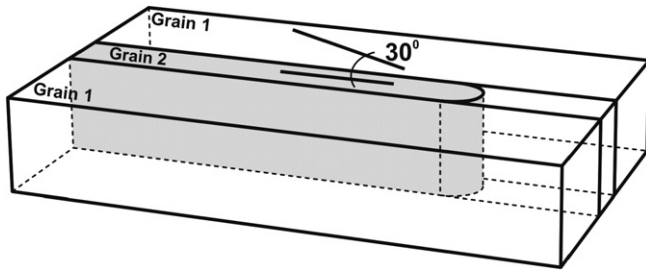 *E-mail address:* Gottstein@imm.rwth-aachen.de (G. Gottstein).

Fig. 1. Scheme of the Zn bicrystal containing the $[10\bar{1}0]$ tilt GBs with misorientation angles of 30°. The lines denote the orientation of basal plane (0001) in both grains.

Fig. 2. Video frame of a moving GB half-loop with facet.

modified Bridgman technique [11,12]. The bicrystals contained two tilt GBs with misorientation 30° $[10\bar{1}0]$. The "special" GB with $\Sigma 15$ is located at $29.9 \pm 0.2°$. Two 30° GBs grew in parallel and eventually formed a half-loop configuration (Fig. 1). Both the flat and curved GB segments were oriented perpendicular to the surface of the sample. The motion of the boundary was observed *in situ* on the hot stage of an optical microscope using polarized light. The shape of the migrating GB half-loop was recorded *in situ* in the temperature range between 633 and 683 K. The temperature was stable within ± 0.5 K during the measurement, and the temperature was increased for consecutive isothermal anneals by 5 or 10 K. Each isothermal anneal took 120 or 180 s; the temperature of the hot stage and the sample stabilized in a few seconds. The samples were protected from oxidation by a pure nitrogen atmosphere. Prior to the measurements the samples were electropolished in a $H_3PO_4 + C_2H_5OH$ solution. In the microscope the reflected beam had to pass a polarization filter to reveal different orientations by different intensities of reflected light. The GB shape was imaged in the course of the experiment by a video camera connected to the microscope and recorded by a VCR.

3. Results

The moving GB half-loop was observed to develop one facet (Fig. 2) at low annealing temperatures. Each curved GB segment connects a facet to the horizontal flat part of the GB. Fig. 3 reveals the moving GB half-loop by a sequence of video frames.

With increasing temperature, the length of the facet l continuously decreased (Fig. 4). At $T = 673$ K the facet disappeared. Above this temperature the GB half-loop comprised only curved segments (Fig. 3). On cooling the facet reappeared again.

In Fig. 5 the dependence of the facet length on the annealing time is shown. The time 0 corresponded to the time when the temperature of the sample and the hot stage became stable after having been raised 5–10 K from the previous annealing temperature. The migration rate of the faceted and non-faceted GB half-loop was found to
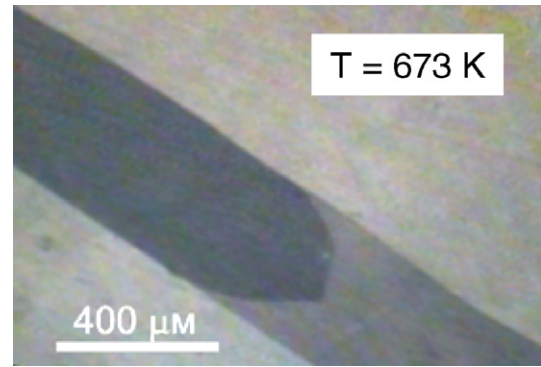
remain constant at a given temperature, which proved that a true steady-state motion was being studied. It is noted that, after the sample temperature had been established, the facet did not reach its stationary length immediately but with a certain delay.

4. Discussion

4.1. Origin of the GB facets

The formation of a GB facet is usually due to a low GB energy for the specific facet inclination. From geometrical arguments, a low GB energy can be associated with a high density of coincidence points of a coincidence site lattice (CSL) [7,13,14]. However, in hexagonal close-packed (hcp) crystals, a three-dimensional coincident site lattice (CSL) can only be obtained when the c/a ratio of the atomic spacing a in the basal plane (0001) and c perpendicular to (0001) is rational [15]. Therefore, an exact CSL exists in Zn only for GBs with $[0001]$ rotation axis. In all other cases, including $[10\bar{1}0]$ tilt GBs, it is necessary to associate the c/a value with the closest rational value to obtain a three-dimensional CSL. This is called a constrained coincidence site lattice (CCSL) [15,16]. This approach allowed a successful description of the observed GB structures in Zn [17,18]. A section of the CCSLs perpendicular to the $[10\bar{1}0]$ tilt axis is shown in Fig. 6 for a GB with a misorientation angle of 30°. Filled and open circles, respectively, mark the lattice points of the two misoriented Zn lattices. Large grey circles mark the CCSL sites. It is obvious that the points of both lattices do not coincide exactly, and the difference may reach a few per cent of the lattice spacing. This situation is similar to near-coincidence GBs of materials with cubic lattice, when the misorientation angle is close but not equal to the misorientation of exact coincidence θ_Σ, although still inside the range for special GBs [11,19]. The reciprocal density of coincidence sites for the studied $\theta = 30°$ $[10\bar{1}0]$ GB is $\Sigma = 17$. Both boundary facet planes form an angle of 76°. One has to bear in mind that the c/a ratio in Zn is temperature dependent [20]. The CCSL shown in Fig. 6 is calculated for 690 K.
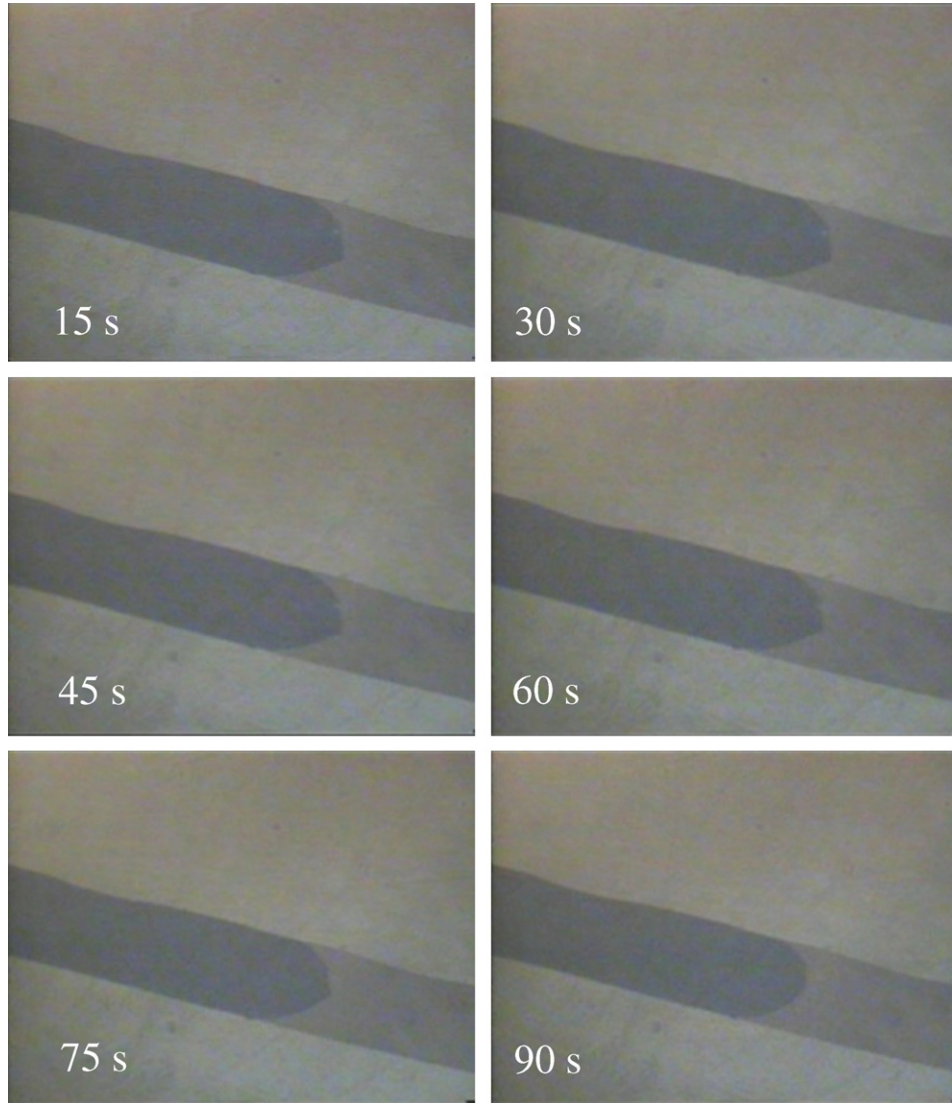
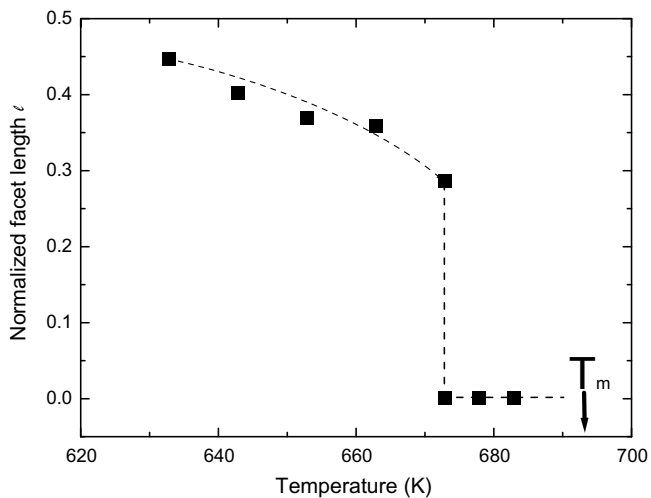Fig. 3. Video frames of GB half-loop motion with and without facet at 673 K.

Fig. 4. Temperature dependence of the facet length *l*.

4.2. Theory of motion of a faceted GB

Let us consider the steady-state motion of a GB half-loop with a facet. A schematic sketch of this faceted boundary is given in Fig. 7. It resembles closely the experimentally observed shape (Figs. 1 and 2).

The equation of motion and the boundary conditions that define the steady-state shape and the velocity V of a moving half-loop are given in Ref. [11]. In the case of a partially faceted boundary, the respective equations of motion and the boundary conditions for the curved boundary read (Fig. 7)

$$Y'' = -\frac{V}{\gamma_b m_b} y'(1 + y'^2),$$

(a) $\quad y'(l\cos\theta) = \tan(\theta - \varphi),$

(b) $\quad y(\infty) = a/2,$ (1)

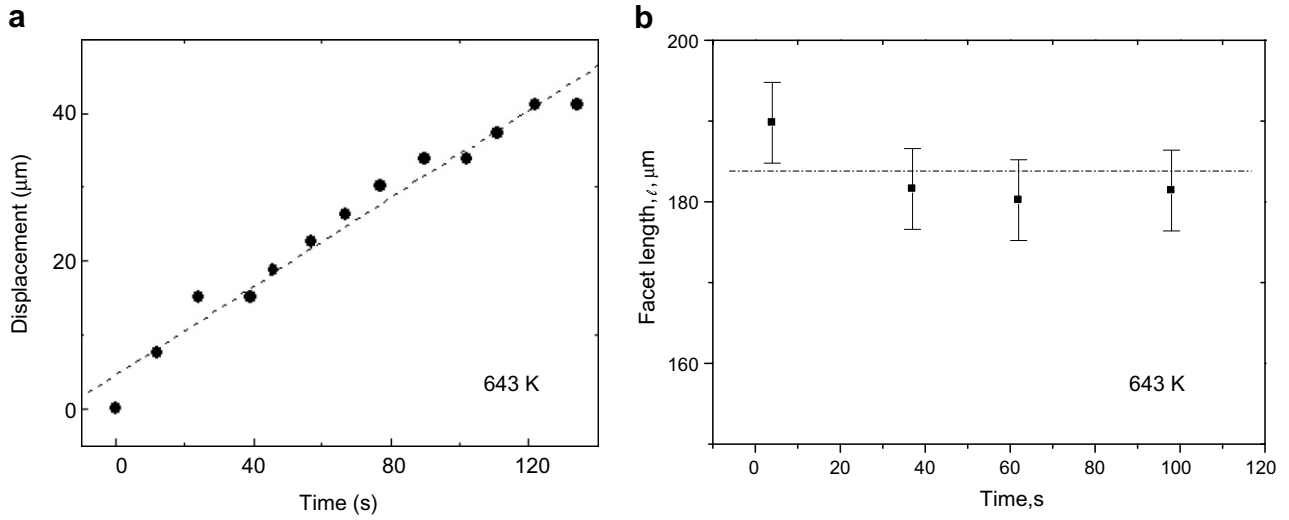(c) $\quad y(l\cos\theta) = l\sin\theta.$

a

b

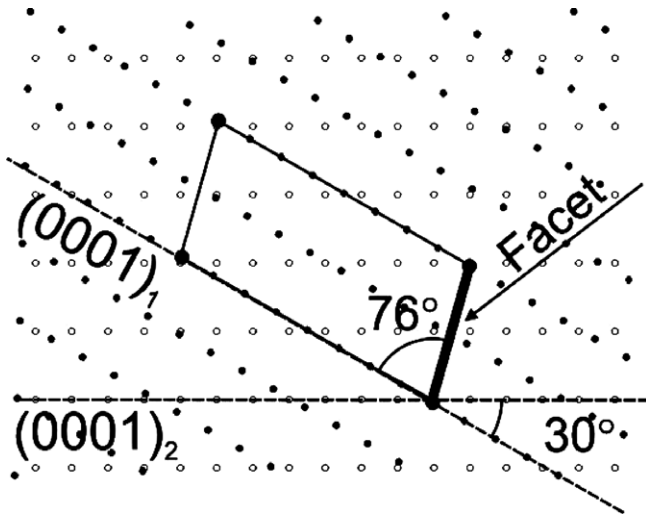Fig. 5. Time dependency of GB half-loop displacement (a) and length of the facet (b).

Fig. 6. Section of CCSL perpendicular to the $[1\,0\,\bar{1}\,0]$ tilt axis for GBs with misorientation angle θ of 30°. Filled and empty circles mark the sites of the two misoriented Zn lattices. Large circles mark CCSL sites. The reciprocal density of coincidence sites is $\Sigma = 17$. The unit cell of the respective CCSL, the position of the basal plane $(0\,0\,0\,1)$ for grain 2 and the CCSL plane parallel to the facet on the moving GB are also shown.

The shape of the moving curved segment of the half-loop without facet is described by a solution of Eq. (1) [11]

(a) $y(0) = 0$,

(b) $y(\infty) = \dfrac{a}{2}$,

(c) $y'(0) = \infty$,

$$y(x) = \frac{a}{2} \arccos\left[\exp\left(-\frac{2\theta}{a}x + \ln(\sin\theta)\right)\right] - \frac{a}{2\theta}\left(\frac{\pi}{2} - \theta\right),$$

$$V = 2\frac{\theta m_b \gamma_b}{a}.$$

$$(2)$$

Here, m_b, γ_b are GB mobility and surface tension, respectively.
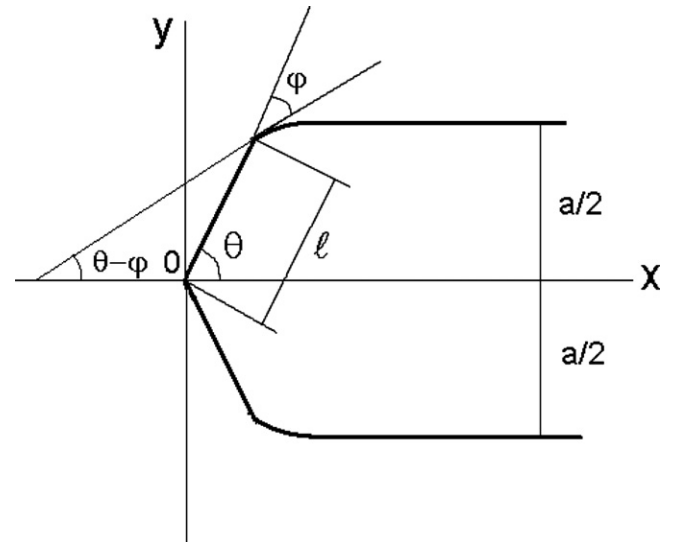

Fig. 7. Geometry of a GB half-loop with a facet.

Since the facet is flat with inclination θ (Fig. 7) the shape of the curved part of the moving half-loop with a facet is given by the equation

$$y = \frac{a}{2} - \frac{m_b\gamma_b}{V}\frac{\pi}{2} + \frac{m_b\gamma_b}{V}$$
$$\times \arccos\left[\sin(\theta - \varphi)\exp\left(\frac{V}{m_b\gamma_b}(l\cos\theta - x)\right)\right]. \quad (3)$$

To determine the velocity of the moving half-loop we draw on boundary condition (c) $y(l\cos\theta) = l\sin\theta$, which yields

$$V = \frac{m_b\gamma_b(\theta - \varphi)}{\frac{a}{2} - l\sin\theta}. \quad (4)$$

Alternatively, to determine the velocity of a faceted GB the approach first put forward by Mullins [21] can be invoked. An infinitesimal grain area change dS due to a moving GB element dl can be expressed as (Fig. 7)

$$ds = m_b \gamma_b \kappa dl = m_b \gamma_b \frac{d\phi}{dl} dl = m_b \gamma_b d\phi,$$

where $\kappa = \frac{d\phi}{dl}$ is the curvature, and

$$\int_0^{\theta - \varphi} m_b \gamma_b d\phi = (\theta - \varphi) m_b \gamma_b = \left(\frac{a}{2} - l \sin \theta\right) V. \qquad (5)$$

Eq. (5) is equivalent to Eq. (4).

Since for a steady-state motion the faceted and curved segments of the half-loop have to move with the same velocity, the migration rate of the GB half-loop with a facet is also controlled by the facet motion. Formally the facet velocity can be expressed as

$$V = m_f \gamma_f \kappa, \qquad (6)$$

where m_f, γ_f are the mobility and surface tension of the facet, respectively.

The magnitude of γ_f determines the equilibrium between curved boundary and facet

$$\gamma_f = \gamma_b \cos \varphi. \qquad (7)$$

The equivalent curvature of the facet κ can be found from the so-called weighted mean curvature approach [9,10]. The weighted mean curvature is defined by the reduction of the total interfacial free energy in the course of an infinitesimal facet displacement divided by the volume swept by the displaced facet. As one can see from the Fig. 7, the infinitesimal displacement of the facet changes the interfacial energy of the system by $\gamma_b \sin \varphi \sin \theta \cdot \delta \cdot dn$, where dn is the normal displacement of the facet, δ is the thickness of the sample, while the volume swept by the facet is equal to $l \cdot \delta \cdot dn$. Then the velocity of the facet can be expressed as (Fig. 7)

$$V = \frac{m_f \gamma_b \sin \varphi \sin \theta}{l}. \qquad (8)$$

Combining Eqs. (4) and (8) yields the length of a moving facet

$$l = \frac{\frac{a}{2}}{\sin \theta + \frac{m_b(\theta - \varphi)}{m_f \sin \varphi \sin \theta}}. \qquad (9)$$

It can be seen that Eq. (9) complies with expectations for the limiting cases. If the mobility of the GB, m_b, is large or the mobility of the facet, m_f, is small, the length of the facet tends to zero. For a facet with a large mobility the length approaches the maximal value $l = \frac{a}{2 \sin \theta}$. If, for instance, the difference between the surface tension of the facet and the curved GB is small – i.e. the angle φ is small – then the second term in the denominator of Eq. (9) increases, and the length of the facet decreases accordingly. The dependency of the normalized facet length $\left(\frac{l}{a/2}\right)$ for different values of the angles φ and θ are given in Fig. 8. It is obvious that the thermodynamic and kinetic factors markedly influence the normalized facet length. The facet length increases with rising angle φ at constant θ as well as with falling θ at constant φ. Eq. (8) gives us the possibility to
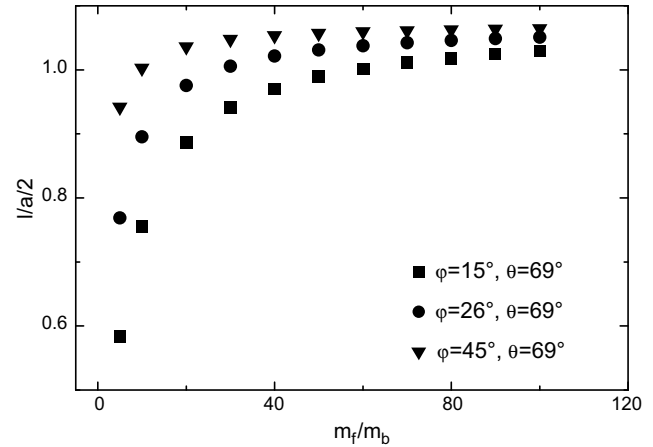

Fig. 8. The dependency of the normalized facet length on the normalized facet mobility for different angles φ and θ.

derive the mobility of the facet and its temperature dependence from the experimentally measured values of the facet length.

The normalized facet mobility (m_f/m_b) extracted from the experimental data and Eq. (9) is presented in Fig. 9. (In the measured temperature range of about 40 K the angle φ remains constant, in the framework of experimental error; in other words, the ratio $\frac{\gamma_f}{\gamma_b}$ is also constant.) A reduction in the facet length with rising temperature is mainly caused by a decrease in the ratio m_f/m_b. On the other hand, the absolute value of the facet mobility can be extracted if the GB mobility is known from an independent experiment. In Ref. [22] the migration of individual non-faceted GBs in zinc was studied. Using such data, we determined the facet mobility (Fig. 10). Apparently, the enthalpy of facet migration is extremely low (~0.1 eV) in our experiments, but corresponds closely to that of the experimentally measured value of the faceted half-loop mobility (~0.15 eV, Fig. 11).

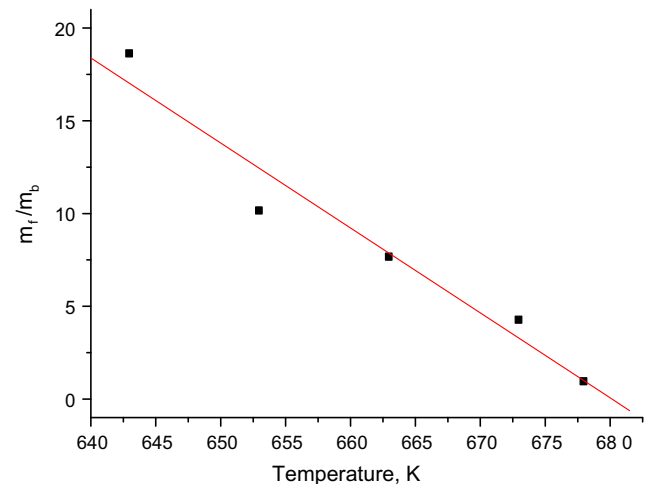Such low enthalpy suggests that the migration of the facet, i.e. displacement rate normal to itself, proceeds

Fig. 9. Temperature dependence of the ratio of the facet normalized mobility m_f/m_b.
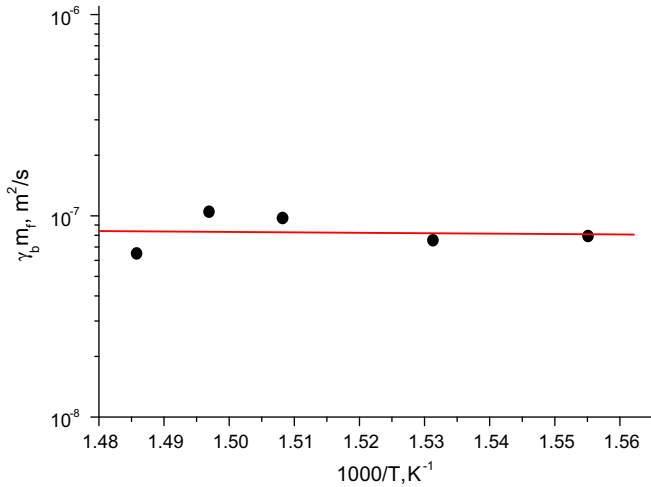
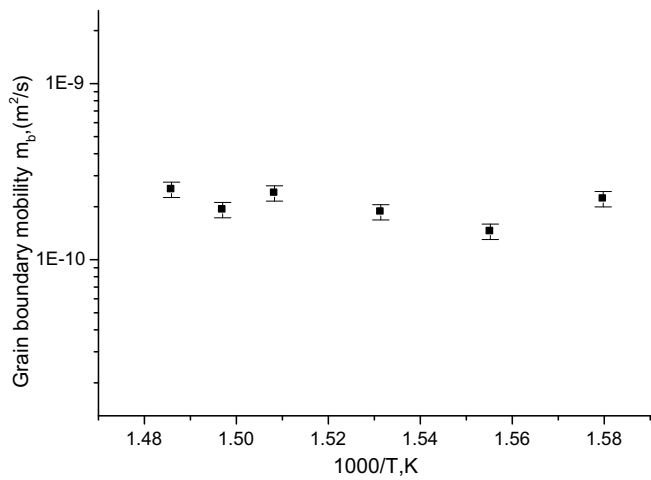Fig. 10. Temperature dependence of the facet mobility.

Fig. 11. Experimentally measured temperature dependence of the GB half-loop motion with facets; the evaluated enthalpy of activation $H \approx 0.1$ eV.

through step motion along the facet. We would like to stress again that the decrease in the facet length is only due to an increase in the mobility of the curved boundary. It is emphasized as well that the value l, as determined by Eq. (9) is the facet length corresponding to a steady-state motion of the faceted half-loop. Our experimental measurements, in particular, the time dependency of the facet length at 673 K, allow us to calculate the GB half-loop displacement as a function of the facet length at constant temperature. Indeed, the velocity of a GB half-loop with facet is determined by the Eqs. (4) and (8). In our calculations we used Eq. (8). In order to apply this equation to our problem we need to know the facet mobility m_f. This quantity can be found from the dependency given in Fig. 9 and experimental data for the reduced mobility $\gamma_b m_b$ for tilt GB $[10\bar{1}0]$ measured in independent experiments [11,22]: $\gamma_b m_b = 1.25 \times 10^{-9} \, \text{m}^2 \, \text{s}^{-1}$ [11,22]. The desired reduced mobility of the facet $\gamma_b \sin \varphi \cdot m_f$ at 673 K was then found to be equal to $6.8 \times 10^{-9} \, \text{m}^2 \, \text{s}^{-1}$. Using the experimental

measured time dependency of the length of the facet at 673 K (Fig. 12b), we determine the GB velocity and, finally, the displacement of the GB half-loop at this temperature. Fig. 12 reveals the time dependency of the facet length l at 673 K (the temperature at which the facet disappears) as well as the measured and calculated value of the GB half-loop displacement. The excellent agreement between the experimental and theoretical data strongly supports the outlined concept. The deviation between the experimental and calculated curves was observed only on the last, rather small, portion of the curve, where there is no longer agreement between the theoretical model and experiment, due to small size of the facet.

4.3. Facet mobility

A surprising result of the current investigation is the high facet mobility with very low activation energy. Moreover, an increase in the facet length with increasing facet mobility seems counterintuitive, since it is a frequent observation that faceted boundaries move with low mobility [1,23]. In this context it is stressed, however, that the
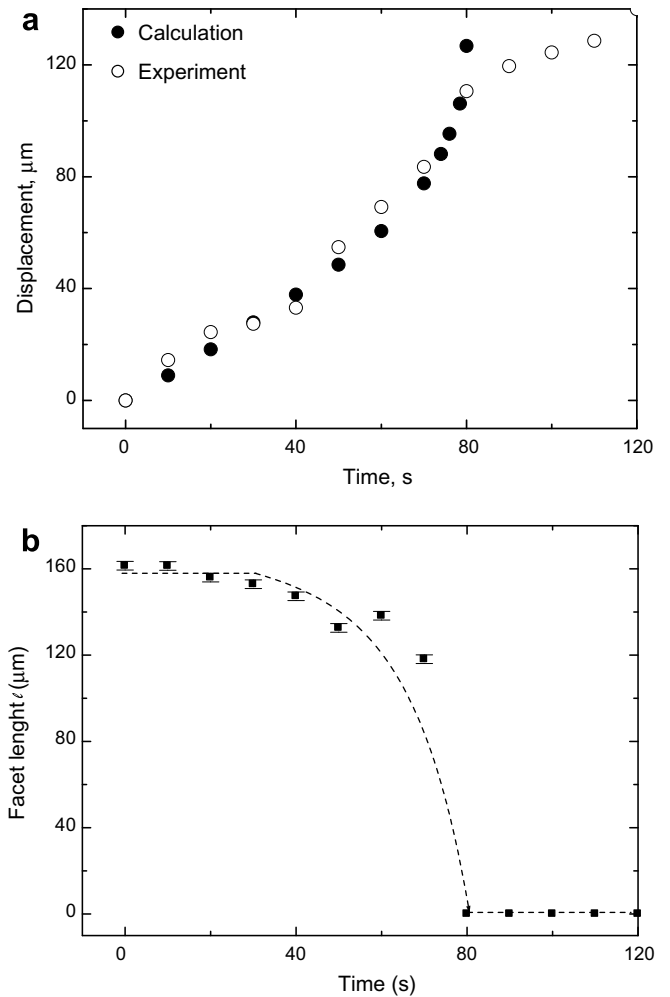

Fig. 12. Measured and calculated displacement of the GB half-loop at 673 K where the facet disappears.

V.G. Sursaeva et al. / Acta Materialia 56 (2008) 2728–2734

steady-state motion of a GB with a facet was investigated in the current study. Correspondingly, the migration rate and the facet length are determined by the respective thermodynamic and kinetic parameters, e.g. materials chemistry or GB energy and mobility. The high mobility of the facet is associated with a low activation energy and is attributed to a high step mobility on the facet. This interpretation tacitly assumes that the production rate of steps on the facet is sufficiently high not to affect the facet velocity. (In particular, it can be assumed that the steps are injected into the facet from the shrinking part of the boundary.) This may not be true, though, for smooth low-energy facets such as coherent twin GBs. In this case the migration rate may be determined by the production rate of steps on the facet rather than by step migration, and consequently, steady-state motion with a facet of finite length may not be possible according to Eq. (9). Yoon and Cho [24] proposed that besides the faceting transition there may also be a roughening transition where smooth facets become rough due to entropy-driven defect generation (steps, vacancies). Accordingly, GBs with facets may reveal quite different thermodynamics and kinetics with changing temperature, as confirmed experimentally [23]. The facet motion studied in the current investigation was obviously observed in a regime where the facet mobility was not constrained by the facet structure so that a steady-state motion of the faceted GB half-loop could be established.

Acknowledgments

References

[1] Gottstein G, Murmann HC, Renner G, Simpson C, Lücke K. In: Gottstein G, Lücke K, editors. Textures of materials. Berlin: Springer-Verlag; 1978. p. 521.
[2] Hsieh TE, Balluffi RW. Acta Metall 1989;37:2133.
[3] Watson GM, Gibbs D, Song S, Sandy AR, Mochril SGJ, Zener DM. Phys Rev 1995;52:12329.
[4] Lee SB, Yoon DY, Henry MB. Acta mater 2000;48:3071.
[5] Koo JB, Yoon DY. Metall Mater Trans A 2001;32:469.
[6] Kazaryan A, Wang Y, Dregia SA, Patton BR. Acta Mater 2002;50:2491.
[7] Straumal BB, Rabkin E, Sursaeva VG, Gornakova AS. Z Metallkd 2005;96:2.
[8] Rabkin E. J Mater Sci 2005;40:875.
[9] Herring C. In: Kingston WE, editor. The physics of powder metallurgy. New York: McGraw-Hill; 1951. p. 143.
[10] Taylor JE. Acta Metall 1992;40:1475.
[11] Gottstein G, Shvindlerman LS. Grain boundary migration in metals: thermodynamics, kinetics, applications. Boca Raton, FL: CRC Press; 1999.
[12] Straumal BB, Sursaeva VG, Gornakova AS. Z Metallkd 2005;96:1147.
[13] Bollmann W. Crystal defects and crystalline interfaces. Berlin: Springer-Verlag; 1970.
[14] Pond RC, Smith DA. Int Met Rev 1976;21:61.
[15] Bruggeman GA, Bishop GH, Hart WH. In: Hu H, editor. The nature and behaviour of grain boundaries. New York, London: Plenum Press; 1972.
[16] Chen FR, King AH. Acta Crystallogr 1987;43:416.
[17] Chen FR, King AH. Philos Mag A 1988;57:431.
[18] Shin K, King AH. Philos Mag A 1991;63:1023.
[19] Straumal BB, Shvindlerman LS. Acta Metall 1985;33:1735.
[20] Nye JF. Physical properties of crystals. Oxford: Clarendon Press; 1964.
[21] Mullins WW. J Appl Phys 1956;27:900.
[22] Antonov AV, Kopetskii ChV, Shvindlerman LS, Sursaeva VG. Sov Phys Dokl 1974;18:736. Antonov AV, Kopetskii ChV, Shvindlerman LS, Sursaeva VG. Preprint of the Institute of Solid State Physics, Chernogolovka, 1972.
[23] Kirch DM, Zhao B, Molodov DA, Gottstein G. Scripta Mater 2007;56:939.
[24] Yoon DY, Cho YK. J Mater Sci 2005;40:861.